Microbiology (2014), **160**, 2794–2806 **DOI** 10.1099/mic.0.083469-0

Metabolic regulation of phytoplasma malic enzyme and phosphotransacetylase supports the use of malate as an energy source in these plant pathogens

Mariana Saigo,[1] Adrián Golic,[1] Clarisa E. Alvarez,[1] Carlos S. Andreo,[1] Saskia A. Hogenhout,[2] María A. Mussi[1] and María F. Drincovich[1]

[1]Centro de Estudios Fotosintéticos y Bioquímicos (CEFOBI- CONICET), Facultad de Ciencias Bioquímicas y Farmacéuticas, Universidad Nacional de Rosario, 2000 Rosario, Argentina

[2]Department of Cell and Developmental Biology, The John Innes Centre, Norwich NR4 7UH, UK

Correspondence
María A. Mussi
mussi@cefobi-conicet.gov.ar
María F. Drincovich
drincovich@cefobi-conicet.gov.ar

Received 16 August 2014
Accepted 3 October 2014

Phytoplasmas ('*Candidatus* Phytoplasma') are insect-vectored plant pathogens. The genomes of these bacteria are small with limited metabolic capacities making them dependent on their plant and insect hosts for survival. In contrast to mycoplasmas and other relatives in the class *Mollicutes*, phytoplasmas encode genes for malate transporters and malic enzyme (ME) for conversion of malate into pyruvate. It was hypothesized that malate is probably a major energy source for phytoplasmas as these bacteria are limited in the uptake and processing of carbohydrates. In this study, we investigated the metabolic capabilities of '*Candidatus* (*Ca.*) phytoplasma' aster yellows witches'-broom (AYWB) malic enzyme (ME). We found that AYWB-ME has malate oxidative decarboxylation activity, being able to convert malate to pyruvate and CO_2 with the reduction of either NAD or NADP, and displays distinctive kinetic mechanisms depending on the relative concentration of the substrates. AYWB-ME activity was strictly modulated by the ATP/ADP ratio, a feature which has not been found in other ME isoforms characterized to date. In addition, we found that the '*Ca.* Phytoplasma' AYWB PduL-like enzyme (AYWB-PduL) harbours phosphotransacetylase activity, being able to convert acetyl-CoA to acetyl phosphate downstream of pyruvate. ATP also inhibited AYWB-PduL activity, as with AYWB-ME, and the product of the reaction catalysed by AYWB-PduL, acetyl phosphate, stimulated AYWB-ME activity. Overall, our data indicate that AYWB-ME and AYWB-PduL activities are finely coordinated by common metabolic signals, like ATP/ADP ratios and acetyl phosphate, which support their participation in energy (ATP) and reducing power [NAD(P)H] generation from malate in phytoplasmas.

INTRODUCTION

Phytoplasmas ('*Candidatus* Phytoplasma') are insect-vectored plant pathogens that produce devastating effects on the yields of high-value agricultural species, such as coconut, grapevine, apple, maize, oilseed rape, carrot, cabbage and onion (Bertaccini, 2007; Hogenhout *et al.*, 2008; Strauss, 2009). Phytoplasmas are obligate parasites that survive and replicate intracellularly within both insects and plant hosts. They are injected into the plants via the feeding activity of an insect vector, and within the plant they inhabit the phloem. Although several aspects of phytoplasma virulence have been revealed in recent years (MacLean *et al.*, 2014; Sugio & Hogenhout, 2012), much less is known on phytoplasma metabolism, an intriguing aspect due to their highly impaired metabolic capabilities as a consequence of the loss of genetic modules. Analyses of five completely sequenced phytoplasma genomes indicated that the utilization of sugars may not be a generalized pathway for energy generation in these bacteria and raised the question about the usage of alternative carbon sources for energy production. Considering the presence of malate transporters in all phytoplasmas, this C_4 acid has been suggested as a possible candidate for such a purpose (Bai *et al.*, 2006; Kube *et al.*, 2012; Oshima *et al.*, 2013). Bearing in mind that phytoplasma infections result in plant nutrient depletion, phytoplasma metabolism

Abbreviations: ACK, acetate kinase; AYWB, aster yellows witches'-broom; ME, malic enzyme; PDHC, pyruvate dehydrogenase complex; PTA, phosphotransacetylase; PTS, phosphotransferase transporter systems.

Two supplementary figures, including a species tree, are available with the online Supplementary Material.

could be critical for their pathogenesis and may contribute to the observed symptoms, such as stunting and dwarfism, typically observed in phytoplasma-infected plants.

Phytoplasmas are members of the class *Mollicutes*, which includes pathogens of eukaryotes (humans, animals and plants) and are thought to have diverged from ancestral low-G+C Gram-positive bacteria from the *Bacillus–Clostridium* group through retrogressive evolution, massive genome reduction and cell wall loss of (Hogenhout *et al.*, 2008; Razin *et al.*, 1998). Unlike other members of the class *Mollicutes*, such as the *Mycoplasmatales* and *Entomoplasmatales*, phytoplasmas do not have hexokinase or phosphotransferase transporter systems (PTS) to import sugars and to generate glucose 6-phosphate to feed glycolysis. In this sense, phytoplasmas are clearly different from the insect-transmitted plant-pathogenic *Spiroplasma citri* or *Spiroplasma kunkelii*, which harbour PTS for the import of fructose, glucose and trehalose (André *et al.*, 2003). In addition, possession of a gene encoding a full-length sucrose phosphorylase, which may compensate for the absence of hexokinase and PTS, is not a general trait in phytoplasmas (Bai *et al.*, 2006; Kube *et al.*, 2012). A functional glycolytic pathway is not present in all phytoplasmas, as in the case of '*Ca.* Phytoplasma mali', which lacks the downstream part of the glycolysis pathway as deduced by bioinformatic analyses (Kube *et al.*, 2008). Furthermore, analyses of five sequenced phytoplasma genomes indicated that these bacteria lack gene sets for sterol biosynthesis, tricarboxylic acid cycle (TCA), *de novo* synthesis of nucleotides and amino acids, ATP synthases and a complete pentose phosphate pathway (Bai *et al.*, 2006; Kube *et al.*, 2012).

Considering that key sugar utilization pathways appear to be absent in phytoplasmas, alternative pathways for energy generation could potentially be operating in these bacteria. According to genome analysis, one potential pathway leading to ATP generation, encoded in all sequenced phytoplasma genomes, would involve malate conversion to acetate (Bai *et al.*, 2006; Kube *et al.*, 2012). Although no experimental evidence for the functionality of this pathway has been provided to date, it is proposed that malate, taken up by the symporter CitS, may be converted to pyruvate by malic enzyme (ME), from pyruvate to acetyl-CoA by the pyruvate dehydrogenase complex (PDHC), from acetyl-CoA to acetyl phosphate by a phosphotransacetylase (PTA), and finally from acetyl phosphate to acetate by an acetate kinase (ACK) (Fig. 1). Genes encoding ME, PDHC and ACK were identified in the phytoplasma genomes, while a gene for a traditional PTA gene was absent. However, it was proposed that PduL, an enzyme involved in B12-dependent 1,2-propanediol degradation in *Salmonella enterica* (Liu *et al.*, 2007), may compensate for the absence of PTA (Kube *et al.*, 2012).

In this study, we performed a detailed biochemical characterization of the product of '*Ca.* Phytoplasma' AYWB_051 open reading frame (AYWB-ME), annotated as a NAD-dependent malic enzyme, and compared its properties to other malic enzymes (MEs). In addition, we characterized the product of AYWB_646 (AYWB-PduL) annotated as a propanediol utilization protein (PduL-like protein). Our work indicated that AYWB-ME and AYWB-PduL constitute key elements in the '*Ca.* Phytoplasma' AYWB malate processing pathway leading to the generation of ATP and NAD(P)H.

METHODS

Bacterial strains and growth media. *Escherichia coli* strain K-12 was used for cloning the open reading frame of AYWB-ME and AYWB-PduL. Strains were routinely cultured aerobically in Luria–Bertani (LB) broth with appropriate antibiotics. *E. coli* strain BL21(DE3) was used for the expression and purification of AYWB-ME and AYWB-PduL.

Cloning, expression and purification of AYWB-ME and -PduL proteins. AYWB-ME and -PduL open reading frames were amplified by PCR using total DNA of '*Ca.* Phytoplasma' AYWB-infected lettuce plants as a template with the following primers: pduLF: 5′-GCTAGCATGGAGGAAAACATGTAT-3′ and pduLR: 5′-CTCGAGTTATTTCAGTAATTTAAC-3′; and AYWBF: 5′-GCTAGCATGAACATCAAAGAAAAAGCAT-3′ and AYWBR: 5′-CTCGAGTCATTTTCTTACTACTCCAGT-3′, which were tailed with *Nhe*I and *Xho*I restriction sites, respectively, in both cases. The amplified products were cloned into pGEM T-Easy (Promega), and the *Nhe*I–*Xho*I fragments were further subcloned into the cognate sites of pET-28a (Novagen). The expression products were designed to contain an N-terminal hexahistidine (6× His) tag for purification on Ni-agarose.

For expression, BL21(DE3) cells transformed with pET-AYWB-ME or pET-AYWB-PduL were grown to a final OD_{600} of 0.4–0.8 in LB medium containing kanamycin. The cultures were then induced by the addition of 0.1 mM IPTG. After 12–16 h of aerobic growth at 16 °C, the cells were harvested by centrifugation for 5 min at 4000 ***g*** and resuspended in buffer A (100 mM Tris/HCl, pH 8.0, 10 mM $MgCl_2$, 2 mM PMSF, 5 mg DNase I ml^{-1}). The lysates obtained by sonication were centrifuged for 20 min at 15 000 ***g*** at 4 °C and the supernatants were mixed with binding buffer 1× (5 mM imidazole, 500 mM NaCl, 20 mM Tris/HCl, pH 7.9) supplemented with glycerol 10 %, v/v. The supernatants (soluble fraction) were loaded onto 5 ml Niquel-NTA columns (Qiagen) previously equilibrated with binding buffer. After washing with binding buffer and washing buffer (49 mM imidazole, 500 mM NaCl, 20 mM Tris/HCl, pH 7.9) the proteins were eluted with elution buffer (200 mM imidazole, 500 mM NaCl, 20 mM Tris/HCl, pH 7.9). The eluted His-tagged AYWB-ME and AYWB-PduL proteins were concentrated (Amicon Ultra-15, Millipore) and desalted using buffer B (100 mM Tris/HCl, pH 7.5, 10 %, v/v, glycerol), then digested with a protein/thrombin ratio of 20 : 1 in buffer B supplemented with 1 mM $MgCl_2$ at 16 °C for 2 h, in order to remove the N terminus encoded by the expression vector. The purified proteins were stored at −80 °C until further characterization. Protein concentrations were determined spectrophotometrically at 280 nm using the theoretical extinction coefficient of each protein: AYWB-ME (8940 M^{-1} cm^{-1}) and AYWB-PduL (3034 M^{-1} cm^{-1}), considering their corresponding predicted protein sequence.

NAD-ME and NADP-ME activity assays. The optimal pH for AYWB-ME was determined using the following three buffers: 50 mM MES (pH 5.5 to 6.5); 50 mM Tricine-MOPS (pH 7.0 to 7.5); and 50 mM Tris/HCl (pH 7.5 to 8.5). The oxidative decarboxylation of L-malate by AYWB-ME was monitored using spectrophotometric assays by adding the substrates NAD or NADP and malate at varying

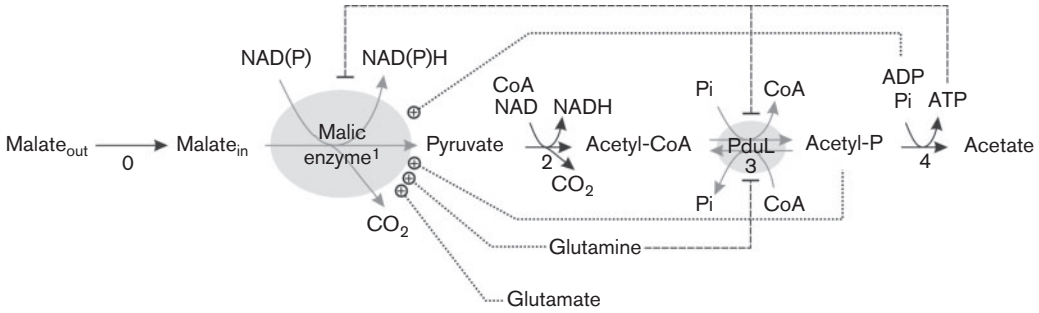

Fig. 1. Proposed pathway for malate utilization in phytoplasmas. The pathway includes the transport of malate from the environment to the cytosol carried out by malate-sodium symporter (CitS, AYWB_52, step 0); the conversion of malate to pyruvate by malic enzyme (ME, AYWB_51, step 1); pyruvate to acetyl-CoA by the pyruvate dehydrogenase complex (PDHC, AYWB_136, AYWB_137, AYWB_138, AYWB_139, step 2); acetyl-CoA to acetyl phosphate by a phosphotransacetylase (PduL, AYWB_646, step 3); and finally, acetyl phosphate to acetate by an acetate kinase (ACK, AYWB_560, step 4). The scheme also shows the regulatory model based on results presented in this study. Dotted and dashed lines indicate activating and inhibiting effects, respectively.

concentrations, in a final volume of 0.5 ml, alongside a standard reaction mixture containing 100 mM Tris/HCl (pH 8.2), 0.25 mM $MnCl_2$ or 5 mM $MgCl_2$. All substrate concentrations reported refer to the free, uncomplexed reactant concentrations, and were calculated considering the dissociation constant of the different complexes formed (Mg^{2+}-NADP, Mn^{2+}-NAD, Mg^{2+}-malate and Mn^{2+}-malate). The reaction was started by the addition of L-malate and the absorbance at 340 nm at 30 °C was instantly recorded. One unit of the enzyme was defined as the amount of enzyme that catalysed the production of 1 μmol NAD(P)H min^{-1}. An absorption coefficient of 6.22 mM^{-1} cm^{-1} for NAD(P)H was used in the calculations. The kinetic parameters were calculated from triplicate experiments and subjected to nonlinear regression using the following equations (Detarsio *et al.*, 2007; Tronconi *et al.*, 2010):

Michaelis–Menten: $v=(V_{max}S)/(K_m+S)$, where S is the substrate concentration, K_m is the Michaelis constant and V_{max} is the maximal velocity;

Hill: $v=(V_{max}S^n)/(S_{0.5}{}^n+S^n)$, where S is the substrate concentration, $S_{0.5}$ is the substrate concentration at the semi-saturation point, n is the Hill coefficient and V_{max} is the maximal velocity;

Two-site: $v=(V_1SK_2+V_2S^2)/(K_1K_2+SK_2+S^2)$, where S is the substrate concentration, K_1 is the dissociation constant of the substrate in the catalytic site, K_2 is the dissociation constant of the substrate in the regulatory site, V_1 is the maximal velocity when the regulatory site is empty and V_2 is the maximal velocity when the regulatory site is occupied.

All data-fitting procedures were performed with the Sigma Plot 11.0 program.

Potential inhibitors or activators of enzyme activity were analysed by measuring AYWB-ME activity at pH 8.2 in the absence or presence of 0.5, 1.0 or 2.0 mM succinate, fumarate, citrate, glucose 6-phosphate, aspartate, glycine, glutamate, glutamine, ADP, ATP or acetyl phosphate; or 20 or 50 μM of CoA or acetyl-CoA. The final pH and metal concentrations were checked after addition of the metabolites and corrected if necessary. The malate concentration used for metabolite assessments was 2 mM, while the concentration of co-factor NAD was 0.05 mM and of co-factor NADP 0.08 mM.

PTA activity assays of AYWB-PduL. PTA activity of AYWB-PduL in the direction of acetyl-CoA synthesis (forward direction) was assayed at 30 °C by monitoring the thioester bond formation of acetyl-CoA at 233 nm (ε_{233nm}=5.55 mM^{-1} cm^{-1}). The assay mixture contained 50 mM Tris/HCl pH 8.0, 20 mM KCl, 10 mM lithium acetyl phosphate, 0.2 mM lithium-CoA and 2 mM dithiothreitol (Bologna *et al.*, 2010). The reverse activity (acetyl phosphate synthesis) was monitored by measuring the phosphate-dependent CoA release from acetyl-CoA with Ellman's thiol reagent, 5′,5-dithiobis(2-nitrobenzoic acid) (DTNB), by measuring the formation of thiophenolate anion at 412 nm (ε_{412nm}=13600 M^{-1} cm^{-1}). The assay mixture contained 50 mM Tris/HCl (pH 8.0), 20 mM KCl, 0.1 mM DTNB, 0.1 mM acetyl-CoA and 5 mM KH_2PO_4 (Bologna *et al.*, 2010). When different compounds were tested as potential inhibitors or activators of phosphotransacetylase activity of AYWB-PduL, both directions of the reaction were measured at pH 8.0 in the absence or presence of 0.5, 2.0 or 4.0 mM of each compound (pyruvate, glutamate, glutamine, alanine, acetate, ATP or ADP). The substrate concentrations were modified to set subsaturating conditions for each reaction: 4 mM CoA and 2 mM acetyl phosphate for the forward direction and 0.02 mM acetyl-CoA for the reverse direction.

Gel filtration chromatography. The molecular mass of the recombinant native AYWB-ME and AYWB-PduL was evaluated by gel filtration chromatography on a fast protein liquid chromatography system with Sephacryl 16/60 200 HR (GE Healthcare Life Sciences). The column was equilibrated with 25 mM Tris/HCl (pH 7.5) and 10 % (v/v) glycerol and calibrated using molecular mass standards. The sample and the standards were applied separately in a final volume of 50 μl at a constant flow rate of 1 ml min^{-1}.

Sequence analyses. Protein sequences were retrieved from nr (non-redundant) databases at NCBI (http://www.ncbi.nlm.nih.gov) and Pfam (Punta *et al.*, 2012), using as query ME or PduL protein sequences from '*Ca.* Phytoplasma asteris' AYWB (AYWB_051 and AYWB_646, respectively) or *E. coli* (SfcA YP_489744 and YP_ 543895, respectively) for bacterial enzymes; or NADP ME from *Arabidopsis thaliana* (At5g11670) for eukaryotic enzymes. For phylogenetic analysis, we included all ME or PduL paralogues present in each organism. The sequences were aligned using CLUSTAL W version 1.7 (Thompson *et al.*, 1994). Gaps were removed from the alignments using BioEdit version 7.05.3 (Hall, 1999). The accession numbers of PDHC and ACK protein sequences present in '*Ca.* P. asteris' AYWB; '*Ca.* Phytoplasma australiense'; '*Ca.* Phytoplasma' OY-M; and '*Ca.* P.

mali' used for distance calculation are as follows: AYWB_136, AYWB_137, AYWB_138, AYWB_139, AYWB_560, PAa_0121, PAa_0686, PAa_0687, PAa_0688, PAa_0689, ATP_00319, ATP_00153, ATP_00154, ATP_00155, ATP_00156, PAM_159, PAM_600, PAM_601, PAM_602 and PAM_603, respectively.

Phylogenetic relationship studies. Phylogenetic relationships were inferred from amino acid sequence alignments using the programs provided in the PHYLIP package, version 3.69 (Felsenstein, 1989) (http://evolution.genetics.washington.edu/phylip.html) and PhyML (Guindon *et al.*, 2010) (http://atgc.lirmm.fr/phyml/). In the case of multimodular ME proteins such as MaeB from *E. coli*, only the module corresponding to ME was extracted from the complete sequences and used for the alignments. The maximum-likelihood (ML) method (PROTML) was used for the construction of the ME domain or PduL phylogenetic tree. In all cases, confidence levels were calculated from 1000 bootstrap resamplings (SEQBOOT) of alignments used for phylogenetic inferences by both neighbour-joining method using a Dayhoff PAM distance matrix (PROTDIST) and the parsimony (PROTPARS) methods, also included in the PHYLIP software package (Felsenstein, 1989).

The RNA phylogenetic tree was constructed using 1467 bp from 16S RNA in the case of bacteria, or from 18S RNA for eukaryotic sequences, using the programs DNAML, DNADIST and DNAPARS contained in the package mentioned above.

RESULTS

AYWB-ME kinetic characterization and metabolic regulation

In silico analysis of the '*Ca.* P. asteris' AYWB genome contents revealed that the full-length putative NAD-dependent ME is encoded by the *AYWB_051* open reading frame (Bai *et al.*, 2006; accession number: NC_007716). This gene is located directly upstream of *AYWB_052*, which encodes a putative malate-sodium symporter (CitS). Both genes are oriented in a head-to-tail fashion (Fig. 2a), suggesting that they may be co-regulated perhaps as an operon. A similar arrangement is present in '*Ca.* P. australiense' and '*Ca.* Phytoplasma' onion yellows genomes. In '*Ca.* P. mali' there are four putative malate/sodium symporters (ATP_00019, ATP_00104, ATP_00151 and ATP_00479); however, they are not close to the putative malic enzyme gene (ATP_00450).

To further functionally characterize the putative AYWB-ME, its coding sequence was amplified and heterologously expressed in *E. coli* to produce a recombinant protein. AYWB-ME was purified to homogeneity showing a monomeric molecular mass of 44 kDa as assessed by SDS-PAGE (Fig. S1, available in the online Supplementary Material). This molecular mass corresponds to the predicted molecular mass based on the AYWB-ME sequence. The native molecular mass of AYWB-ME was calculated by size exclusion chromatography. The value obtained (76.0 ± 9.9 kDa) indicated that AYWB-ME assembles as a dimer, consistent with other MEs that also assemble as dimers (Saigo *et al.*, 2004) or tetramers through the dimerization of dimers (Xu *et al.*, 1999).

AYWB-ME activity measurements with L-malate as a substrate and in the presence of the co-factors NAD or NADP and either Mn^{2+} or Mg^{2+} revealed malate oxidative decarboxylation activity, with maximum activity at pH 8.2 (Fig. S1). Subsequent kinetic studies were performed in the presence of NAD-Mn^{2+} or NADP-Mg^{2+}, which are typical conditions for NAD and NADP-ME activity measurements (Saigo *et al.*, 2004; Tronconi *et al.*, 2010) at the optimum pH (8.2). When NAD-dependent ME activity was assessed at varying NAD concentrations (from 0.01 to 2.5 mM), the data fitted to a sigmoid curve according to the Hill equation at low malate concentration (0.09 mM) and to a hyperbolic curve according to Michaelis–Menten equation at high malate concentration (30 mM) (Table 1, Fig. 3). Malate saturation curves in the presence of varying malate concentrations from 0.23 to 37 mM fitted the Hill equation at a low NAD concentration (0.1 mM) and a 2 : 2 rational polynomial (two-site equation; Detarsio *et al.*, 2007) at a high NAD concentration (1.5 mM), with the latter reflecting a two-site binding mechanism with an inhibitory effect of the second binding (Table 1, Fig. 3). When the data were fitted to a kinetic model mechanism, the best score was obtained with the Bi-Ter steady-state random mechanism that allows the sequential binding of the substrates regardless of the order. The results demonstrate malate inhibition at high concentrations, suggesting that AYWB-ME prefers to bind NAD first, though the existence of an allosteric malate-binding site cannot be ruled out.

NADP-dependent AYWB-ME activities were also measured. When malate varied from 0.2 to 32 mM, malate saturation curves fitted to a hyperbolic curve according to the Michaelis–Menten equation at low NADP concentration (0.05 mM) and a 2 : 2 rational polynomial at high NADP concentration (2.3 mM) (Table 1, Fig. 3). However, in contrast to NAD, the NADP saturation curves were non-hyperbolic at neither low (0.2 mM) nor high (30 mM) malate concentrations (Table 1, Fig. 3). Instead, both datasets fitted to a 2 : 2 rational polynomial, which can be interpreted as a two-site binding model with an activating effect of the second NADP molecule binding. In this case, the non-hyperbolic behaviour cannot be explained by a kinetic mechanism, but rather the data suggest that AYWB-ME adopts an allosteric regulatory mechanism in the presence of NADP.

To evaluate the response of AYWB-ME to different metabolic intermediates, possibly relevant for activity modulation in the plant host, the NAD- and NADP-dependent activities of AYWB-ME were assayed at subsaturating levels of the substrates (2 mM malate and 0.05 mM NAD or 2 mM malate and 0.08 mM NADP), in the presence of different metabolic intermediates at two different concentrations (Fig. 4). These experiments indicated that the NAD-dependent reaction of AYWB-ME increased in the presence of the amino acids glutamate, glutamine, aspartate and glycine (Fig. 4a). The strongest activator was obtained in the presence of 0.5 mM glutamate, which increased AYWB-ME

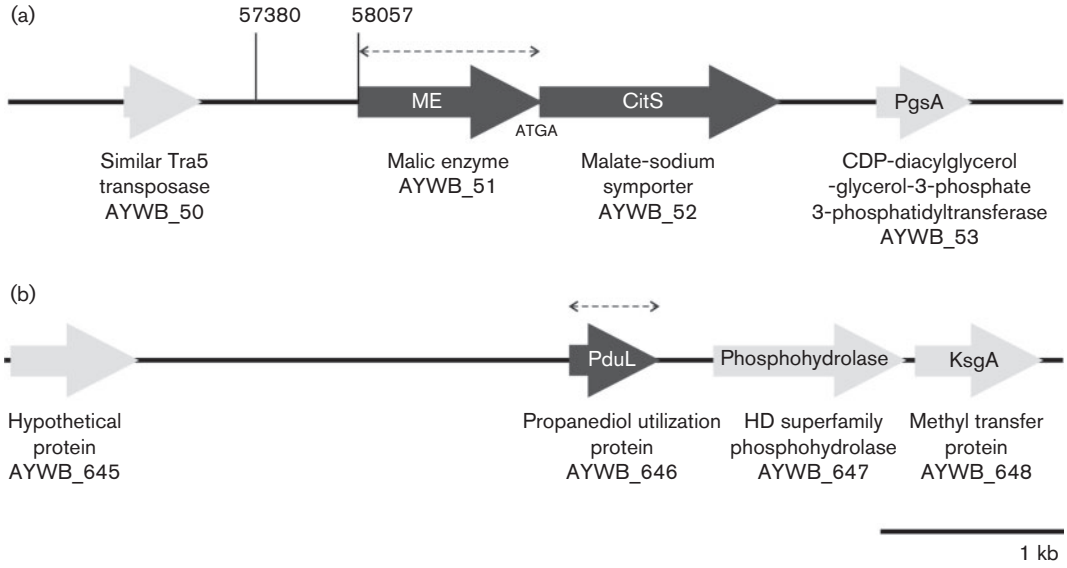

Fig. 2. Genetic organization of the '*Ca.* P. asteris' strain AYWB chromosomal loci containing the gene coding for ME (a) or PduL (b) and flanking regions. Dashed lines indicate the coding regions cloned in expression vectors. Bar, 1 kb.

activity by almost 5-fold, while 0.5 mM glutamine and aspartate activated AYWB-ME by 1.5- and 1.3-fold, respectively. In the presence of 0.5 mM ADP and acetyl phosphate, the AYWB-ME reaction showed an increase of 1.6- and 3.5-fold, respectively. However, 2.0 mM ATP decreased AYWB-ME activity by 40 %. Succinate, fumarate, citrate, acetyl-CoA, CoA, glucose 6-phosphate and acetate did not show any significant effect on AYWB-ME activity.

Table 1. Kinetic parameters of recombinant AYWB-ME

Enzymic activity was determined at various concentrations of one substrate and fixed concentrations of the other (0.02, 0.09 or 30 mM L-malate; 0.1 or 1.5 mM NAD; 0.05 or 2.3 mM NADP) at optimum pH 8.2. The kinetic parameters were estimated by fitting the enzymic measurements to Michaeles–Menten, Hill or two-site model equations. Typical kinetic saturation curves of each case are shown in Fig. 3.

AYWB NAD-dependent malic enzyme activity			
0.09 mM malate		30 mM malate	
K_{NAD}* (mM)	k_{cat} (s^{-1})	K_{NAD}† (mM)	k_{cat} (s^{-1})
0.09 ± 0.003	0.56 ± 0.01	0.12 ± 0.01	10.4 ± 0.11
0.1 mM NAD		1.5 mM NAD	
K_{malate}‡ (mM)	k_{cat} (s^{-1})	K_{malate}§ (mM)	k_{cat} (s^{-1})
1.60 ± 0.20	5.36 ± 0.22	3.67 ± 0.61	15.3 ± 1.21
AYWB NADP-dependent malic enzyme activity			
0.2 mM malate		30 mM malate	
K_{NADP}§ (mM)	k_{cat} (s^{-1})	K_{NADP}§ (mM)	k_{cat} (s^{-1})
0.20 ± 0.12	0.25 ± 0.10	0.23 ± 0.10	3.78 ± 0.85
0.05 mM NADP		2.3 mM NADP	
K_{malate}† (mM)	k_{cat} (s^{-1})	K_{malate}§ (mM)	k_{cat} (s^{-1})
3.19 ± 0.47	0.98 ± 0.03	15.6 ± 8.97	19.9 ± 8.53

*$S_{0.5}$ (Hill equation, $n_H = 1.36 \pm 0.05$).
†K_m (Michaelis–Menten equation).
‡$S_{0.5}$ (Hill equation, $n_H = 1.42 \pm 0.25$).
§K_1 (two-site model equation).

In the NADP-dependent reaction of AYWB-ME, only glutamate and glutamine among the amino acids showed activation effects (3.0- and 1.3-fold, respectively, at 2 mM of each metabolite). In the presence of 2 mM ADP and 2 mM acetyl phosphate, the NADP-dependent AYWB-ME activity was increased almost 6- and 5-fold, respectively, while 2 mM ATP exerted an inhibitory effect (Fig. 4b). As in the NAD-dependent reaction, succinate, fumarate, citrate, acetyl-CoA, CoA, glucose 6-phosphate and acetate did not significantly affect the activity of AYWB-ME in the presence of NADP.

AYWB-ME sequence and phylogenetic analysis

Genes encoding MEs were also found in other completely sequenced phytoplasma genomes. '*Ca.* P. asteris' AYWB-ME shows 96 % identity with '*Ca.* Phytoplasma' onion yellows ME, 78 % with '*Ca.* Phytoplasma solani' and '*Ca.* P. australiense' MEs and 66 % with '*Ca.* P. mali' ME. In addition, ME genes were also found in the draft genomes of milkweed yellows phytoplasma, vaccinia witches'-broom phytoplasma, Italian clover phyllody phytoplasma, poinsettia branch-inducing phytoplasma and peanut witches'-broom phytoplasma, where AYWB-ME shows between 65.2 and 67.2 % identity. The phylogenetic relationships of phytoplasma ME proteins were assessed within bacterial and eukaryotic members of the ME family (Fig. 5). ME sequences group into two distinct clusters, arbitrarily designated clusters 1 and 2 (Fig. 5). Cluster 1 contains the ME sequences from eukaryotes conforming a monophyletic cluster with MEs from both Gram-negative and Gram-positive bacteria. Phytoplasmas MEs belong to cluster 2 along with MEs from various prokaryotes, but not eukaryotes. Notably, no ME homologues were identified in the genomes of other members of the class *Mollicutes*, such as species belonging to the genera *Acholeplasma*, *Spiroplasma*, *Anaeroplasma*, *Mycoplasma, Mesoplasma* or *Ureaplasma* (Figs S2 and 5). The positioning of the phytoplasma ME clade within the cluster comprising MEs from *Clostridium*-like bacteria is in agreement with the notion that phytoplasmas have evolved from a *Clostridium*-like ancestor and matches phylogenetic trees of 16S rDNA sequences (Fig. S2) and multiple sets of concatenated core housekeeping proteins (Zhao *et al.*, 2005). Therefore, it is most likely that phytoplasmas have kept their ME genes during gene loss events rather than acquired them by horizontal gene transfer from other bacteria. In contrast, other members of the *Mollicutes* appear to have lost their ME genes (Chen *et al.*, 2012; Lo *et al.*, 2013). This indicates that phytoplasmas are unique among the *Mollicutes* for their ability to utilize malate.

AYWB-PduL kinetic characterization and metabolic regulation

PduL was first described as having PTA activity in the B12-dependent 1,2-propanediol degradation pathway of *Salmonella enterica* Serovar Typhimurium LT2 (Liu *et al.*, 2007). Kinetic analysis of this enzyme showed that PduL can catalyse the conversion of propionyl-P to propionyl-CoA and, to a much lesser extent, converts acetyl phosphate to acetyl-CoA (Liu *et al.*, 2007). Here, we evaluated whether AY-WB phytoplasma PduL encoded by *AYWB_646* converts acetyl-CoA to acetyl phosphate in the malate utilization pathway (Fig. 1).

AYWB-PduL was cloned and heterologously expressed in *E. coli* to produce the recombinant protein. Purified AYWB-PduL has a monomeric molecular mass of 22 kDa corresponding to the predicted molecular mass based on its sequence. The native molecular mass of AYWB-PduL was calculated by size exclusion chromatography. The value obtained (42.6 ± 0.5 kDa) indicates that AYWB-PduL assembles as a dimer.

The purified AYWB-PduL was used for enzymic activity measurements. This indicated that AYWB-PduL catalyses the conversion of acetyl phosphate to acetyl-CoA with a k_{cat} of 10.8 ± 2.0 s^{-1}, which is in the same range as the k_{cat} of 5.4 s^{-1} of *Sal. enterica* PduL. AYWB-PduL also catalyses the conversion of acetyl-CoA to acetyl phosphate with a k_{cat} of 6.26 ± 0.64 s^{-1}. However, this activity was not measured in the case of *Sal. enterica* PduL.

Next, we assayed AYWB-PduL activity at subsaturating levels of the substrates (4 mM CoA and 2 mM acetyl phosphate for the forward reaction, and 0.02 mM acetyl-CoA for the reverse reaction) in the presence of different metabolites. Among the compounds tested (glutamate, glutamine, ATP, ADP, pyruvate and acetate), only ATP and glutamine showed modulation of AYWB-PduL activity. The addition of 4 mM ATP lowered the velocity of the conversion of acetyl-CoA to acetyl phosphate from 6.1 ± 0.4 to 4.7 ± 0.1 U mg^{-1}, whereas it did not modify the opposite reaction. Conversely, 2 mM glutamine lowered the velocity of the conversion of acetyl phosphate to acetyl-CoA from 11.9 ± 0.6 to 9.0 ± 0.1 U mg^{-1}, yet this amino acid did not modify the opposite reaction. In the presence of 2 mM pyruvate, both reactions were activated to a similar extent, without a net stimulation in a particular direction of the reaction. Therefore, AYWB-PduL displays metabolite-regulated PTA activity in both the direct and reverse reactions.

Phylogenetic relationships of AYWB-PduL

PduL is prevalent in prokaryotes, while homologues have not been found in members of the *Archaea* or *Eukarya* (Liu *et al.*, 2007). The PduL-like coding gene does not appear to be part of an operon structure, but lies upstream of genes encoding a putative phosphohydrolase and a methyltransferase in the genome of the '*Ca.* Phytoplasma' AYWB (Fig. 2b). Phosphohydrolases and methyltransferases play important roles in signalling and in the metabolism of nucleotides (Zimmerman *et al.*, 2008). AYWB-PduL homologues were found in all sequenced phytoplasma genomes, in *Acholeplasma laidlawii* and in some species of mycoplasmas such as *Mycoplasma* sp. CAG776 (Fig. S2,

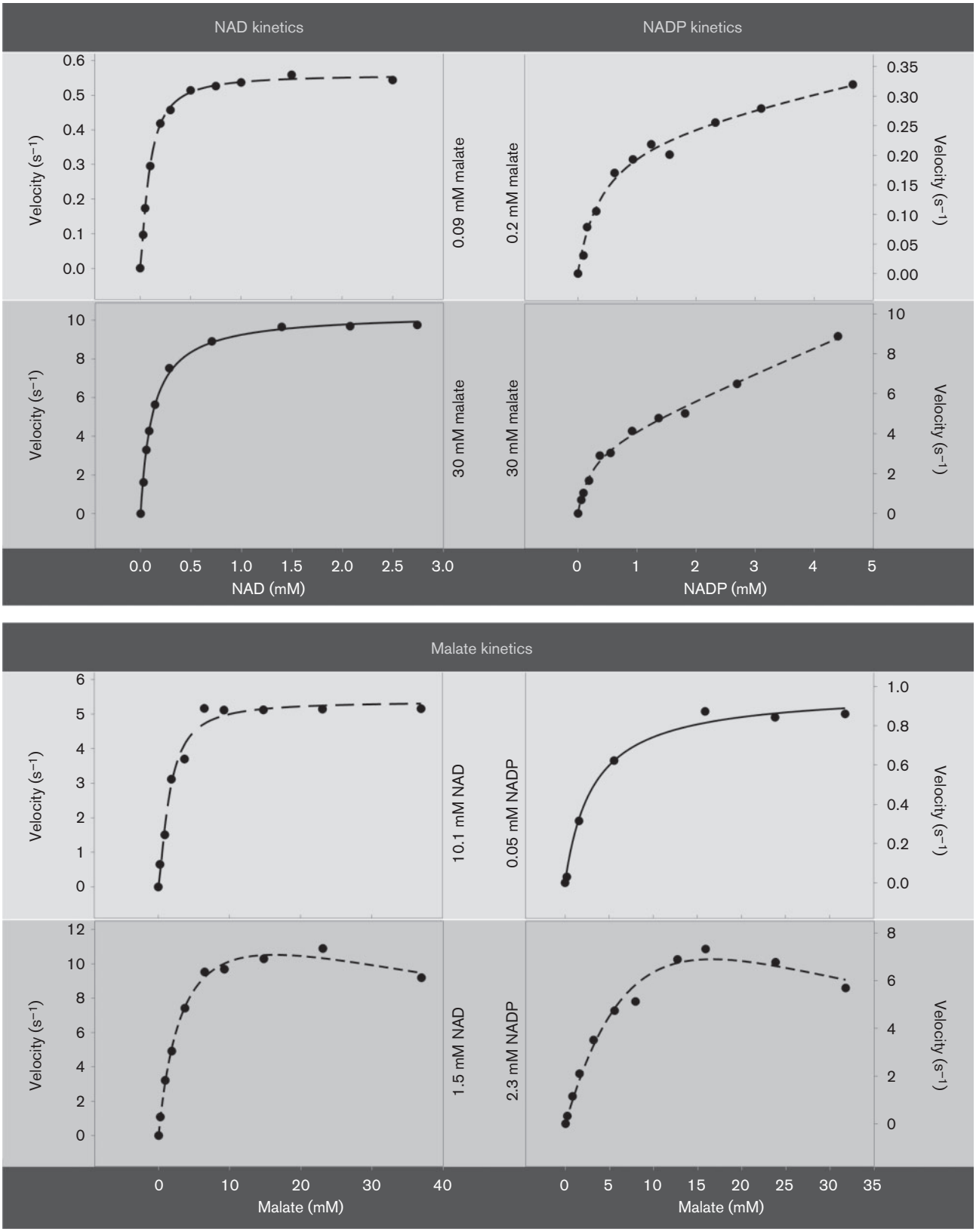

Fig. 3. Typical saturation curves of AYWB-ME activity at different substrate concentrations. Upper panels: NAD- (left) and NADP-dependent AYWB-ME activity (right) were determined at various concentrations of NAD or NADP, respectively, and at fixed low or high malate concentration. The fixed concentrations of malate are indicated in each graph. Lower panels:

NAD- (left panels) and NADP-dependent AYWB-ME activity (right panels) were determined at various concentrations of malate and at fixed low or high NAD(P) concentration. The fixed concentrations of NAD or NADP are indicated in each graph. The saturation curves were fitted to Michaelis–Menten (solid lines), Hill (long dashed lines) or two-site (short dashed lines) model equations and the estimated kinetic parameters obtained with the best-fitted equation are indicated in Table 1. Typical results from at least three independent determinations, which showed the same fitting results, are shown.

underlined; Fig. 6) but not in other species such as *Mycoplasma feliminutum*, *Mycoplasma hominis* or other non-mycoplasma members within the *Mollicutes* such as *Anaeroplasma varium*, *Ureaplasma urealyticum*, *Mesoplasma florum* or the insect-transmitted phytopathogen *Spi. citri* (Fig. S2). Overall, phylogenetic analysis shows that phytoplasma and mycoplasma PduL sequences share a monophyletic origin (Fig. 6). These PduL sequences are in close proximity and appear to share a monophyletic cluster with species belonging to the *Bacillus–Clostridium* group, consistent with the 16S rDNA phylogenetic tree (Fig. S2). Therefore, similarly to the ME genes, it is unlikely that the PduL genomic region has been acquired by horizontal gene transfer, but has been maintained in the phytoplasma genomes despite reductive genome evolution.

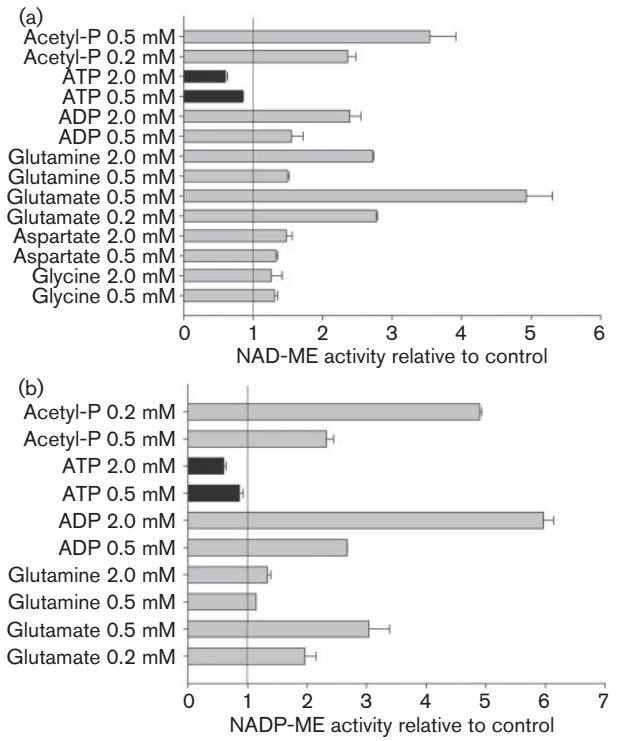

Fig. 4. Regulatory properties of AYWB-ME. NAD-dependent (a) and NADP-dependent (b) AYWB-ME activity were measured at pH 8.2 in the absence or presence of the effectors indicated in the y-axes. The activity measured in the presence of each effector is expressed relative to the activity measured in their absence. Assays were performed at least in triplicate and error bars indicate ± SD. Inhibition effects are indicated in black (ratios lower than 1) and activation effects in grey (ratios lower than 1).

Other components of the putative malate utilization pathway in phytoplasmas

In the putative pathway proposed for malate utilization in phytoplasmas (Fig. 1), ME is followed by PDHC composed of three components in phytoplasmas: pyruvate decarboxylase (E1α and E1β subunits), dihydrolipoamide acetyltransferase (E2) and dihydrolipoamide dehydrogenase (E3), that would convert pyruvate to acetyl-CoA. The four subunits of PDHC are highly conserved between '*Ca.* P. asteris' AYWB and '*Ca.* Phytoplasma' onion yellows (93 to 98 % identity among the different components). '*Ca.* P. australiense' PDHC subunits display 71 to 85 % identities with corresponding subunits from '*Ca.* P. asteris' AYWB and '*Ca.* Phytoplasma' onion yellows. '*Ca.* P. mali' PDHC subunits are the most divergent, showing 53 to 69 % identities with those of '*Ca.* P. asteris' AYWB, '*Ca.* Phytoplasma' onion yellows and '*Ca.* P. australiense'. The four subunits of PDHC are arranged in close proximity in these four phytoplasma genomes, most likely constituting an operon.

The last steps in the putative pathway proposed for malate utilization in phytoplasmas (Fig. 1) involve acetyl-CoA conversion to acetate with the production of ATP through the combination of PTA, followed by ACK (Fig. 1). Regarding ACK proteins, sequence distances show a similar pattern to PDHC subunits. In particular, the ACK protein encoded in '*Ca.* P. asteris' AYWB shows 95 % identity with the homologue of '*Ca.* Phytoplasma' onion yellows, 73 % with that of '*Ca.* P. australiense' and 61 % with that of '*Ca.* P. mali'. Therefore, all components of the malate utilization pathway, as shown in Fig. 1, are likely to be represented in all phytoplasmas.

DISCUSSION

Malate to acetate: a conserved pathway for ATP and reducing power generation in phytoplasmas

Two key phytoplasma proteins, ME and PduL, were functionally characterized in this study. Both proteins function in the malate metabolism pathway that produces energy in the form of ATP and NAD(P)H as reducing power (Fig. 1). Firstly, the results demonstrate that ME, encoded by AYWB_051, has malate oxidative decarboxylation activity, being able to convert malate to pyruvate and

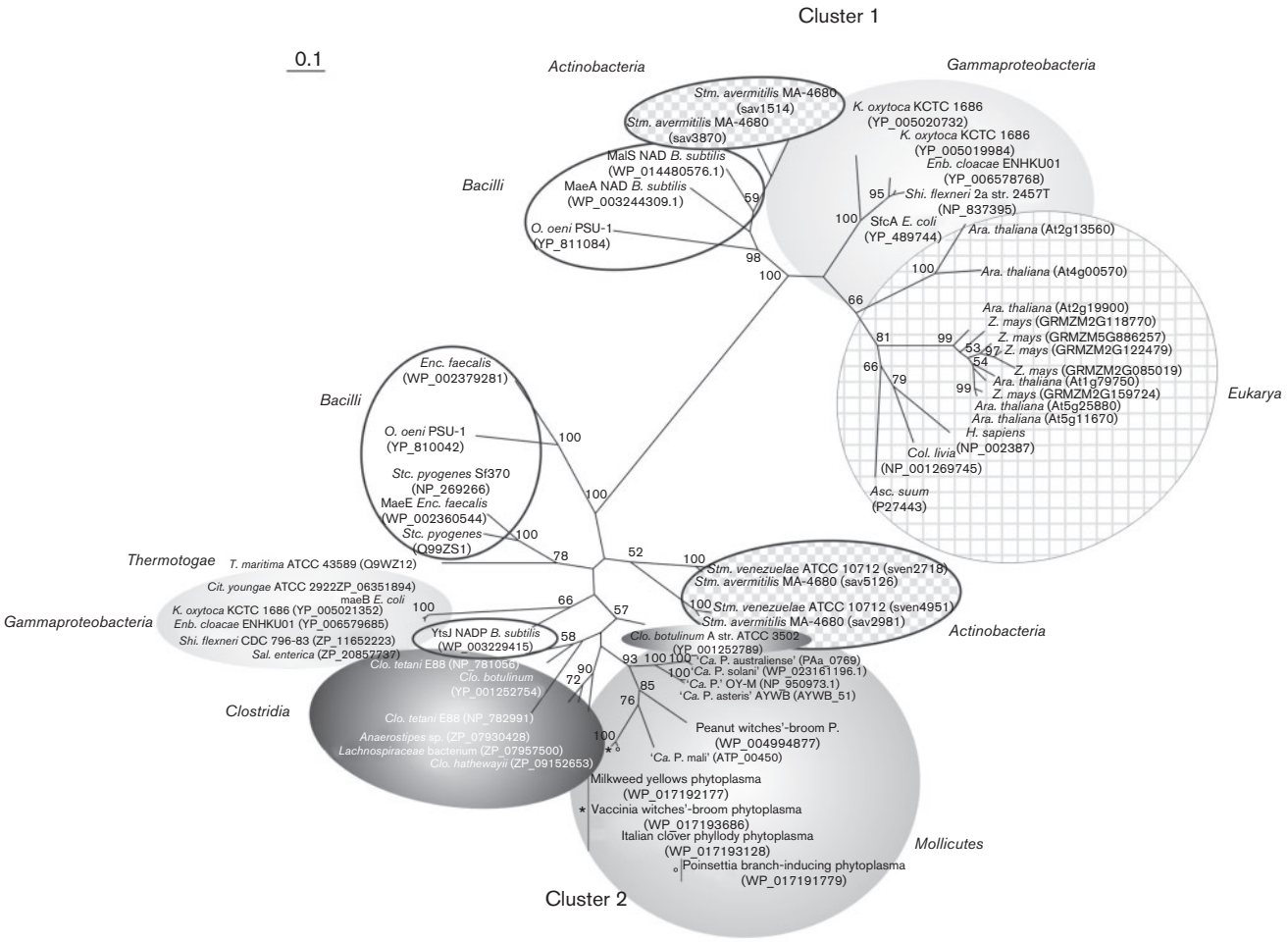

Fig. 5. Phylogenetic relationships of members of the ME family found in different taxa such as bacteria and eukaryotes. The complete set of sequences of MEs from *Zea mays* and *Ara. thaliana*, and protein sequences whose structures have been solved such as *Homo sapiens* mitochondrial NADP-ME (Xu *et al.*, 1999; Yang & Tong, 2000), *Columba livia* cytosolic NADP-ME (Yang *et al.*, 2002a, b), *Ascaris suum* NAD-ME (Coleman *et al.*, 2002), *Streptococcus pyogenes* serotype M1 NAD- ME (Beres *et al.*, 2002) and *Thermotoga maritima* strain ATCC 43589 NAD-ME (Nelson *et al.*, 1999), among other bacterial sequences less characterized, were included. The tree was constructed using the maximum-likelihood method as implemented in PhyML. Branch support values are derived from 100 bootstrap replicates; only values greater than 50 % are shown. Two clusters (C1 and C2) supported by bootstrap values are indicated. Circles with different shadings are used to differentiate clusters of MEs from different types of organism: *Bacilli* class (Gram-positive); *Clostridia* class (Gram-positive); *Gammaproteobacteria* class (Gram-negative); *Mollicutes*; *Actinobacteria* (Gram-positive); eukaryotes. Sequences from the following additional organisms were used: *Bacillus subtilis*; '*Ca.* P. asteris' AYWB; '*Ca.* P. australiense'; '*Ca.* Phytoplasma onion yellows strain M ('*Ca.* P.' OY-M); '*Ca.* P. mali'; *Citrobacter youngae*; *Clostridium botulinum*; *Clostridium tetani*; *Clostridium hathewayi*; *Enterobacter cloacae*; *Enterococcus faecalis*; *Escherichia coli*; *Klebsiella oxytoca*; *Oenococcus oeni*; *Sal. enterica*; *Shigella flexneri*; *Streptococcus pyogenes*; *Streptomyces avermitilis*; *Streptomyces venezuelae*; *Oenococcus oeni*.

CO_2 with the concomitant reduction of either NAD to NADH or NADP to NADPH (Fig. 1). Secondly, AYWB-ME activity was found to be modulated by the energetic status of the cell represented by the ATP/ADP ratio. At low ATP/ADP ratios, ME is activated to supply pyruvate for further oxidation coupled with ADP phosphorylation and concomitant generation of energy in the form of ATP, while at high ATP/ADP ratios ATP inhibits the activity of ME (Fig. 1). Thirdly, this study shows that PduL encoded by AYWB_646 (annotated as PduL-like enzyme) effectively harbours PTA activity, being able to convert acetyl-CoA to acetyl phosphate (Fig. 1). PduL is therefore likely to function in the malate utilization pathway rather than in the propanediol degradation pathway, in agreement with the absence of other genes of the propanediol pathway in phytoplasmas, such as *pduCDE*, *pduQ*, *pduP* and *pduW* (Kube *et al.*, 2012). Finally, the regulation of PduL phosphotransacetylase activity by ATP and glutamine, as

occurs with ME, agrees with a concerted role of PduL with ME in the conversion of malate to acetate (Fig. 1).

It is noteworthy that genes coding for MEs, as well as genes for other enzyme constituents of the malate pathway (Fig. 1), are encoded in all sequenced phytoplasma genomes, in contrast to other members within the *Mollicutes* such as spiroplasmas and mycoplasmas, which lack this set of genes (Fig. S2) (Bai *et al.*, 2006). This fact supports the hypothesis that ME could potentially play a key role in these organisms and therefore has resisted elimination by reductive evolution, as has probably occurred in other members within the *Mollicutes* which harbour a different metabolic repertoire to produce energy or carbon sources. In this context, it is interesting to mention that in *Bacillus subtilis*, the closest walled relative of the *Mollicutes*, malate is the second preferred carbon source after glucose, suggesting that phytoplasmas, as well as *B. subtilis*, have retained the ability to use malate from a common ancestor (Kleijn *et al.*, 2010). This theory is reinforced by the sprinkled appearance of PduL homologues among organisms representative of different classes and, in particular, its absence in most *Mollicutes* with selective retention in phytoplasmas. Therefore, it is likely that selective pressure contributed to the selective maintenance of different metabolic gene sets in different members of the classes *Clostridia*, *Bacilli* and *Mollicutes*, once present in the common ancestor, in concordance with the different lifestyles pursued by these organisms. This might explain why taxonomic and phylogenetic inferences are somewhat misleading for organisms of this group, especially the *Mollicutes*, as these methods are severely dependent on the marker considered.

Metabolic regulation: a strategy to modulate malate utilization in phytoplasmas

Firmicutes, such as *Enterococcus faecalis*, possess two-component systems to regulate malate utilization (Mortera *et al.*, 2012). Such two-component systems are not found in phytoplasmas, indicating that these bacteria use other strategies to regulate malate utilization. We found that AYWB-ME displays unique and complex interactions with its substrates, exhibiting differential kinetic behaviours depending on the relative concentration of malate to NAD(P) (Fig. 3, Table 1). Moreover, different kinetic behaviour is observed even when comparing NAD to NADP, suggesting that these co-factors may signal a differential AYWB-ME response, most likely due to binding to specific allosteric sites. Regarding inhibition of the enzyme at high malate concentrations, this is potentially a strategy to avoid excessive acetate accumulation, which may be toxic to the cells, and could be mediated through allosteric sites for malate in AYWB-ME. In addition, AYWB-ME activity is also modulated by several relevant metabolites, including ATP and ADP, amino acids and acetyl phosphate, produced as a result of PduL activity (Figs 1 and 4).

In bacteria, MEs generally participate in the central metabolism linking TCA and glycolysis/gluconeogenesis (Bologna *et al.*, 2007; Meyer & Stülke, 2013). For example, ME of *B. subtilis* is involved in keeping ATP levels high mainly by supplying NADH to the respiratory chain (Meyer & Stülke, 2013). However, in phytoplasmas the main role of ME is to supply pyruvate to a pathway that generates ATP, explaining the ATP/ADP regulation of AYWB-ME. Activity inhibition by ATP has been documented for ME from prokaryotes (Espariz *et al.*, 2011; Kawai *et al.*, 1996) and eukaryotes (Wheeler *et al.*, 2008; Yang *et al.*, 2002a). However, regulation by both ATP and ADP has not been reported for MEs to date.

The interaction of ATP with human NAD(P)-ME (hNAD(P)-ME) has received much attention due to the relevance of this enzyme in glutamine metabolism in proliferating tumours (Jiang *et al.*, 2013; Yang *et al.*, 2002a). Crystallographic and kinetic analyses have shown that ATP exerts its inhibitory action by binding to the catalytic site of hNAD(P)-ME, and that a NAD molecule binds to a non-catalytic site using the ADP portion of the co-factor (Xu *et al.*, 1999). In this study the activation of AYWB_ME by ADP and NADP was demonstrated, most likely by binding to allosteric sites within this enzyme. ADP is possibly the major source of AYWB-ME activation, as phytoplasmas lack a NAD kinase for production of NADP and can only produce NAD (Kube *et al.*, 2012). Future studies may focus on AYWB-ME crystallography in the presence of ADP to discover novel structural features of this singular ME.

AYWB-ME could potentially adopt different kinetics depending on the environment of the bacteria. Such flexibility is required given that phytoplasmas inhabit diverse environments, including the intracellular phloem sieve cells of plant hosts and the gut lumen, intracellular environments, haemolymph and saliva of insect hosts. For example, glutamate and glutamine, two abundant amino acids in the phloem of several plant species (Kube *et al.*, 2012; Valle *et al.*, 1998; Weibull *et al.*, 1990), may activate AYWB-ME (Fig. 1) when phytoplasmas grow inside the plant host. In this context, transcriptomic and proteomic analyses performed on tissue samples from *Nicotiana occidentalis* infected by '*Ca.* P. mali' strain AT showed evidence of expression of malate/sodium symporter (*mlep*), malic enzyme (*sfcA*), pyruvate dehydrogenase complex (*acoA*, *acoB*, *aceF* and *lpD*), phosphotransacetylase (*pduL*) and acetate kinase (*ackA*) genes. Additionally, it was established that the *sfcA* transcript is more abundant than *pduL* and *ackA* transcripts. This observation and the extensive regulation of AYWB-ME by metabolic effectors found in this study agree with the role of malic enzyme in catalysing the first committed step in the oxidation of malate in phytoplasmas (Siewert *et al.*, 2014). Another interesting case of a plant-associated bacterium in which malic enzyme plays a central role in the metabolism of malate is the symbiotic bacterium *Sinorhizobium meliloti*. In this organism the reduction of the level of a particular malic enzyme (DME) impairs N_2 fixation capacity, suggesting that the conversion of malate to pyruvate is

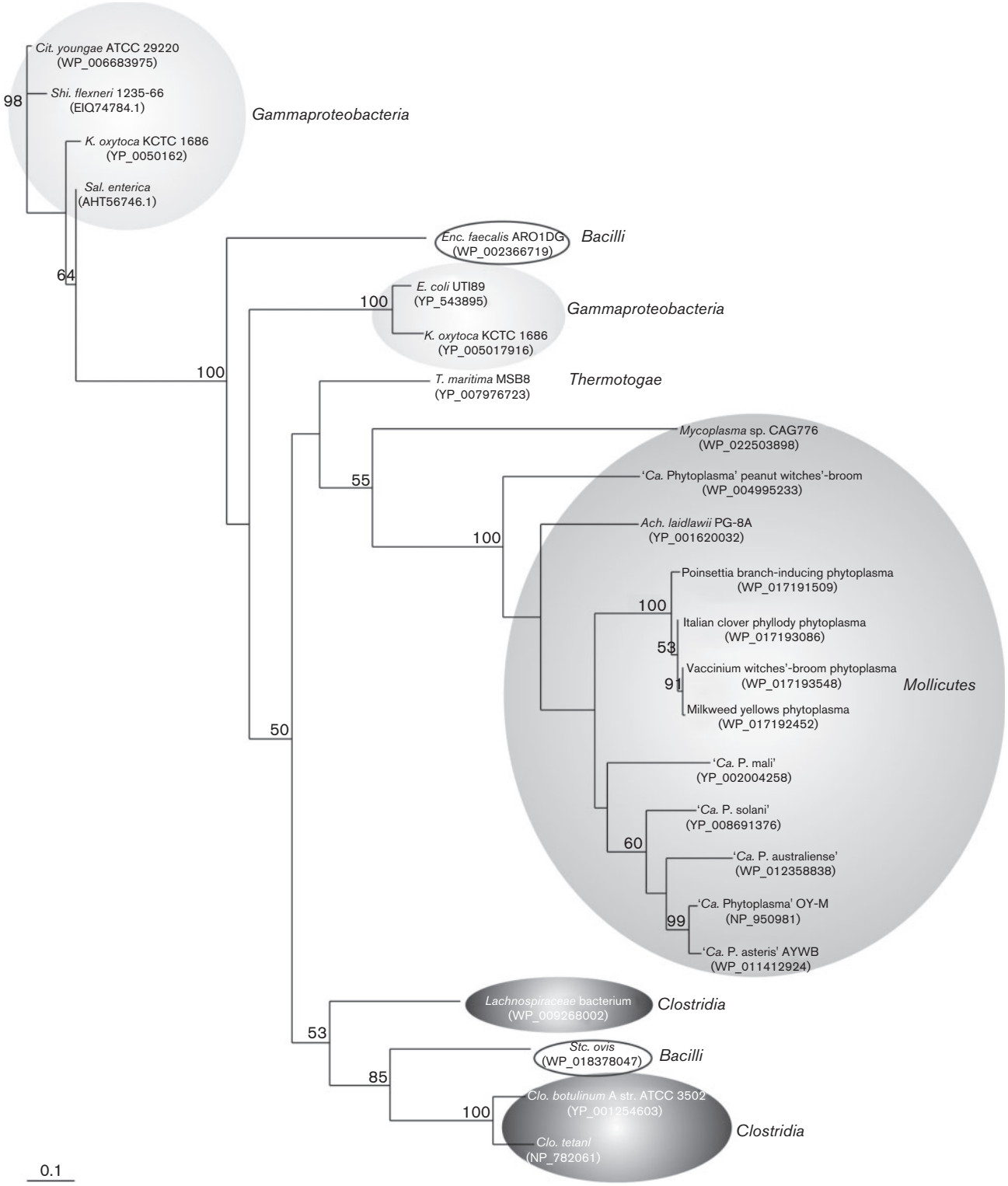

Fig. 6. Phylogenetic relationships of PduL proteins found in bacteria. The tree was constructed using the maximum-likelihood method as implemented in PhyML. Branch support values are derived from 100 bootstrap replicates; only values greater than 50 % are shown. Species names are indicated following the same nomenclature as in Fig. 5. Species not mentioned in Fig. 5 include: '*Ca.* Phytoplasma' peanut witches'-broom; *Ach. laidlawii*; '*Ca.* P. solani'; *Streptococcus ovis*.

required in alfalfa bacteroids to supply carbon and/or energy to the N_2 fixation process (Mitsch *et al.*, 2007). Taken together, the complex kinetics of AYWB-ME in response to various substrates, co-factors and products highlights the importance of a fine regulation of malate utilization in phytoplasma. This involves rapid allosteric sensing of the concentration of key metabolites by this first enzyme of the malate metabolic route (Fig. 1), most likely indicating the particular environment of the bacteria.

ACKNOWLEDGEMENTS

M. S., C. E. A., C. S. A., M. A. M. and M. F. D. are members of the Researcher Career of Consejo Nacional de Investigaciones Científicas y Técnicas (CONICET, Argentina) and A. G. is a fellow of the same institution. We thank Dr Krissana Kowitwanich and Dr Allyson MacLean for their contribution to this work. This work has been supported by the National Agency for Promotion of Science and Technology (ANPCyT) and CONICET.

REFERENCES

André, A., Maccheroni, W., Doignon, F., Garnier, M. & Renaudin, J. (2003). Glucose and trehalose PTS permeases of *Spiroplasma citri* probably share a single IIA domain, enabling the spiroplasma to adapt quickly to carbohydrate changes in its environment. *Microbiology* **149**, 2687–2696.

Bai, X., Zhang, J., Ewing, A., Miller, S. A., Jancso Radek, A., Shevchenko, D. V., Tsukerman, K., Walunas, T., Lapidus, A. & other authors (2006). Living with genome instability: the adaptation of phytoplasmas to diverse environments of their insect and plant hosts. *J Bacteriol* **188**, 3682–3696.

Beres, S. B., Sylva, G. L., Barbian, K. D., Lei, B., Hoff, J. S., Mammarella, N. D., Liu, M. Y., Smoot, J. C., Porcella, S. F. & other authors (2002). Genome sequence of a serotype M3 strain of group A *Streptococcus*: phage-encoded toxins, the high-virulence phenotype, and clone emergence. *Proc Natl Acad Sci U S A* **99**, 10078–10083.

Bertaccini, A. (2007). Phytoplasmas: diversity, taxonomy, and epidemiology. *Front Biosci* **12**, 673–689.

Bologna, F. P., Andreo, C. S. & Drincovich, M. F. (2007). *Escherichia coli* malic enzymes: two isoforms with substantial differences in kinetic properties, metabolic regulation, and structure. *J Bacteriol* **189**, 5937–5946.

Bologna, F. P., Campos-Bermudez, V. A., Saavedra, D. D., Andreo, C. S. & Drincovich, M. F. (2010). Characterization of *Escherichia coli* EutD: a phosphotransacetylase of the ethanolamine operon. *J Microbiol* **48**, 629–636.

Chen, L.-L., Chung, W.-C., Lin, C.-P. & Kuo, C.-H. (2012). Comparative analysis of gene content evolution in phytoplasmas and mycoplasmas. *PLoS ONE* **7**, e34407.

Coleman, D. E., Rao, G. S., Goldsmith, E. J., Cook, P. F. & Harris, B. G. (2002). Crystal structure of the malic enzyme from *Ascaris suum* complexed with nicotinamide adenine dinucleotide at 2.3 A resolution. *Biochemistry* **41**, 6928–6938.

Detarsio, E., Alvarez, C. E., Saigo, M., Andreo, C. S. & Drincovich, M. F. (2007). Identification of domains involved in tetramerization and malate inhibition of maize C_4-NADP-malic enzyme. *J Biol Chem* **282**, 6053–6060.

Espariz, M., Repizo, G., Blancato, V., Mortera, P., Alarcón, S. & Magni, C. (2011). Identification of malic and soluble oxaloacetate decarboxylase enzymes in *Enterococcus faecalis*. *FEBS J* **278**, 2140–2151.

Felsenstein, J. (1989). PHYLIP-phylogeny inference package (version 3.2). *Cladistics* **5**, 164–166.

Guindon, S., Dufayard, J. F., Lefort, V., Anisimova, M., Hordijk, W. & Gascuel, O. (2010). New algorithms and methods to estimate maximum-likelihood phylogenies: assessing the performance of PhyML 3.0. *Syst Biol* **59**, 307–321.

Hall, T. A. (1999). BioEdit: a user-friendly biological sequence alignment editor and analysis program for Windows 95/98/NT. *Nucleic Acids Symp Ser* **41**, 95–98.

Hogenhout, S. A., Oshima, K., Ammar, D., Kakizawa, S., Kingdom, H. N. & Namba, S. (2008). Phytoplasmas: bacteria that manipulate plants and insects. *Mol Plant Pathol* **9**, 403–423.

Jiang, P., Du, W., Mancuso, A., Wellen, K. E. & Yang, X. (2013). Reciprocal regulation of p53 and malic enzymes modulates metabolism and senescence. *Nature* **493**, 689–693.

Kawai, S., Suzuki, H., Yamamoto, K., Inui, M., Yukawa, H. & Kumagai, H. (1996). Purification and characterization of a malic enzyme from the ruminal bacterium *Streptococcus bovis* ATCC 15352 and cloning and sequencing of its gene. *Appl Environ Microbiol* **62**, 2692–2700.

Kleijn, R. J., Buescher, J. M., Le Chat, L., Jules, M., Aymerich, S. & Sauer, U. (2010). Metabolic fluxes during strong carbon catabolite repression by malate in *Bacillus subtilis*. *J Biol Chem* **285**, 1587–1596.

Kube, M., Schneider, B., Kuhl, H., Dandekar, T., Heitmann, K., Migdoll, A. M., Reinhardt, R. & Seemüller, E. (2008). The linear chromosome of the plant-pathogenic mycoplasma '*Candidatus* Phytoplasma mali'. *BMC Genomics* **9**, 306.

Kube, M., Mitrovic, J., Duduk, B., Rabus, R. & Seemüller, E. (2012). Current view on phytoplasma genomes and encoded metabolism. *ScientificWorldJournal* **2012**, 1-25.

Liu, Y., Leal, N. A., Sampson, E. M., Johnson, C. L., Havemann, G. D. & Bobik, T. A. (2007). PduL is an evolutionarily distinct phosphotransacylase involved in B12-dependent 1,2-propanediol degradation by *Salmonella enterica* serovar typhimurium LT2. *J Bacteriol* **189**, 1589–1596.

Lo, W.-S., Chen, L.-L., Chung, W.-C., Gasparich, G. E. & Kuo, C.-H. (2013). Comparative genome analysis of *Spiroplasma melliferum* IPMB4A, a honeybee-associated bacterium. *BMC Genomics* **14**, 22.

MacLean, A. M., Orlovskis, Z., Kowitwanich, K., Zdziarska, A. M., Angenent, G. C., Immink, R. G. & Hogenhout, S. A. (2014). Phytoplasma effector SAP54 hijacks plant reproduction by degrading MADS-box proteins and promotes insect colonization in a RAD23-dependent manner. *PLoS Biol* **12**, e1001835.

Meyer, F. M. & Stülke, J. (2013). Malate metabolism in *Bacillus subtilis*: distinct roles for three classes of malate-oxidizing enzymes. *FEMS Microbiol Lett* **339**, 17–22.

Mitsch, M. J., Cowie, A. & Finan, T. M. (2007). Malic enzyme cofactor and domain requirements for symbiotic N_2 fixation by *Sinorhizobium meliloti*. *J Bacteriol* **189**, 160–168.

Mortera, P., Espariz, M., Suárez, C., Repizo, G., Deutscher, J., Alarcón, S., Blancato, V. & Magni, C. (2012). Fine-tuned transcriptional regulation of malate operons in *Enterococcus faecalis*. *Appl Environ Microbiol* **78**, 1936–1945.

Nelson, K. E., Clayton, R. A., Gill, S. R., Gwinn, M. L., Dodson, R. J., Haft, D. H., Hickey, E. K., Peterson, J. D., Nelson, W. C. & other authors (1999). Evidence for lateral gene transfer between Archaea and bacteria from genome sequence of *Thermotoga maritima*. *Nature* **399**, 323–329.

Oshima, K., Maejima, K. & Namba, S. (2013). Genomic and evolutionary aspects of phytoplasmas. *Front Microbiol.* **4**, 230.

Punta, M., Coggill, P. C., Eberhardt, R. Y., Mistry, J., Tate, J., Boursnell, C., Pang, N., Forslund, K., Ceric, G. & other authors (2012). The Pfam protein families database. *Nucleic Acids Res* **40** (Database issue), D290–D301.

Razin, S., Yogev, D. & Naot, Y. (1998). Molecular biology and pathogenicity of mycoplasmas. *Microbiol Mol Biol Rev* **62**, 1094–1156.

Saigo, M., Bologna, F. P., Maurino, V. G., Detarsio, E., Andreo, C. S. & Drincovich, M. F. (2004). Maize recombinant non-C_4 NADP-malic enzyme: a novel dimeric malic enzyme with high specific activity. *Plant Mol Biol* **55**, 97–107.

Siewert, C., Luge, T., Duduk, B., Seemüller, E., Büttner, C., Sauer, S. & Kube, M. (2014). Analysis of expressed genes of the bacterium '*Candidatus* phytoplasma Mali' highlights key features of virulence and metabolism. *PLoS ONE* **9**, e94391.

Strauss, E. (2009). Microbiology. Phytoplasma research begins to bloom. *Science* **325**, 388–390.

Sugio, A. & Hogenhout, S. A. (2012). The genome biology of phytoplasma: modulators of plants and insects. *Curr Opin Microbiol* **15**, 247–254.

Thompson, J. D., Higgins, D. G. & Gibson, T. J. (1994). CLUSTAL W: improving the sensitivity of progressive multiple sequence alignment through sequence weighting, position-specific gap penalties and weight matrix choice. *Nucleic Acids Res* **22**, 4673–4680.

Tronconi, M. A., Gerrard Wheeler, M. C., Maurino, V. G., Drincovich, M. F. & Andreo, C. S. (2010). NAD-malic enzymes of *Arabidopsis thaliana* display distinct kinetic mechanisms that support differences in physiological control. *Biochem J* **430**, 295–303.

Valle, E. M., Boggio, S. B. & Heldt, H. W. (1998). Free amino acid composition of phloem sap and growing fruit in *Lycopersicon esculentum*. *Plant Cell Physiol* **39**, 458–461.

Weibull, J., Ronquist, F. & Brishammar, S. (1990). Free amino acid composition of leaf exudates and phloem sap: a comparative study in oats and barley. *Plant Physiol* **92**, 222–226.

Wheeler, M. C., Arias, C. L., Tronconi, M. A., Maurino, V. G., Andreo, C. S. & Drincovich, M. F. (2008). *Arabidopsis thaliana* NADP-malic enzyme isoforms: high degree of identity but clearly distinct properties. *Plant Mol Biol* **67**, 231–242.

Xu, Y., Bhargava, G., Wu, H., Loeber, G. & Tong, L. (1999). Crystal structure of human mitochondrial NAD(P)(+)-dependent malic enzyme: a new class of oxidative decarboxylases. *Structure* **7**, 877–889.

Yang, Z. & Tong, L. (2000). Structural studies of a human malic enzyme. *Protein Pept Lett* **7**, 287–296.

Yang, Z., Lanks, C. W. & Tong, L. (2002a). Molecular mechanism for the regulation of human mitochondrial NAD(P)+-dependent malic enzyme by ATP and fumarate. *Structure* **10**, 951–960.

Yang, Z., Zhang, H., Hung, H. C., Kuo, C.-C., Tsai, L. C., Yuan, H. S., Chou, W. Y., Chang, G. G. & Tong, L. (2002b). Structural studies of the pigeon cytosolic NADP(+)-dependent malic enzyme. *Protein Sci* **11**, 332–341.

Zhao, Y., Davis, R. E. & Lee, I. M. (2005). Phylogenetic positions of '*Candidatus* Phytoplasma asteris' and *Spiroplasma kunkelii* as inferred from multiple sets of concatenated core housekeeping proteins. *Int J Syst Evol Microbiol* **55**, 2131–2141.

Zimmerman, M. D., Proudfoot, M., Yakunin, A. & Minor, W. (2008). Structural insight into the mechanism of substrate specificity and catalytic activity of an HD-domain phosphohydrolase: the 5′-deoxyribonucleotidase YfbR from *Escherichia coli*. *J Mol Biol* **378**, 215–226.

Edited by: F. Sargent